

# Chapter 38

## Experimental Study on Failure Mechanisms of Novel Visco-Hyperelastic Material Target Under Ballistic Impact Conditions



**Pawel Zochowski, Marcin Cegla, Marcin Bajkowski, Roman Grygoruk, Mariusz Magier, Krzysztof Szczurowski, Jędrzej Maczak, Mirosław Bocian, Roman Gieleta, and Krzysztof Jamroziak**

**Abstract** The main aim of the study was to define the static and dynamic properties of novel visco-hyperelastic material and its behavior under  $7.62 \times 25$  mm Full Metal Jacket (FMJ) projectile impact condition. Mechanical tests were performed in both quasi-static and dynamic conditions. Uniaxial quasi-static compression tests were performed at different temperatures in order to characterize the influence of thermal effects on the plastic flow of the material. The Split Hopkinson Pressure Bar (SPHB) apparatus was used to assess strain rate sensitivity of the novel material. Residual velocity of projectiles (after perforation of the target) was recorded during the test allowing to evaluate energy absorption and dissipation capability of the visco-hyperelastic layer. The material is intended to be used in different ballistic applications such as projectile catching systems and anti-ricochet layers covering walls of shooting ranges, ballistic tunnels.

**Keywords** Ballistic impact · Numerical simulation · Failure

---

P. Zochowski · M. Cegla

Military Institute of Armament Technology, Wyszyńskiego 7, 05-220 Zielonka, Poland

M. Bajkowski · R. Grygoruk · M. Magier

Institute of Mechanics and Printing, Faculty of Mechanical and Industrial Engineering, Warsaw University of Technology, Narbutta 85, 02-524 Warsaw, Poland

K. Szczurowski · J. Maczak

Institute of Vehicles, Faculty of Automotive and Construction Machinery Engineering, Warsaw University of Technology, Narbutta 84, 02-524 Warsaw, Poland

M. Bocian · K. Jamroziak (✉)

Department of Mechanics, Materials Science and Engineering, Faculty of Mechanical Engineering, Wrocław University of Science and Technology, Smoluchowskiego 25, 50-370 Wrocław, Poland

e-mail: [krzysztof.jamroziak@pwr.edu.pl](mailto:krzysztof.jamroziak@pwr.edu.pl)

R. Gieleta

Faculty of Mechanical Engineering, Military University of Technology, Kaliskiego 2 St., 00-908 Warsaw, Poland

## 38.1 Introduction

Hyperelastic rubber-like materials have been widely used in various engineering applications. Specific features of those materials makes them very effective when used as damping layers or shock absorbers [1–4]. Efficiency of hyperelastic tissue simulants was confirmed in numerous studies of ballistic impact phenomenon [5–7]. When hyperelastic materials are included in the study they become even more complicated due to high elastic recovery of rubbers and temporary character of their deformations. Rubbers and gels can significantly deform under mechanical load and return to their nearly original shape when the load is removed. The rubber-like materials show a highly non-linear stress-strain-deformation relationship in the deformation range above 5%. Even with the use of sophisticated measuring techniques the amount of information that can be collected during ballistic tests on rubber-like materials is often significantly limited due to the nature of the phenomenon and properties of materials. Firstly, the mechanical experiments characterizing the response of the material to the applied loads in a wide range of strain rates were carried out.

## 38.2 Material Characterization Tests

### 38.2.1 *Quasi-Static Compression Tests*

*The novel material is a* elastomer based on modified silicones. The material density is about  $900 \text{ kg/m}^3$ . First of all, compressive response of the target material (conditioned at 293 K) at quasi-static strain rates was examined. Cylindrical samples of 20 mm in height and 19.5 mm in diameter were tested. Tests were registered with a camera in order to record the values of specimens diameter that was changing together with the movement of jaws due to the barreling effect caused by friction at specimen/jaws interfaces. The tests of the mechanical properties of the projectile and target materials were carried out on a Zwick Z100 universal testing machine with a hydraulic drive. The compression process was shown in Fig. 38.1.

The results of quasi-static compression tests of the target material were shown in Fig. 38.2. The actual stresses and strains determined in this way were affected with some errors (omission of the value of correction methods, e.g. by the Bridgmann correction coefficient). However, the influence of these errors on the behavior of numerical models of materials was checked during the validation process.

### 38.2.2 *Dynamic Compression of Hyperelastic Target Material*

The samples from the visco-hyperelastic material were cut with a waterjet cutting machine and then milled to the required thickness. Samples for SHPB tests were made

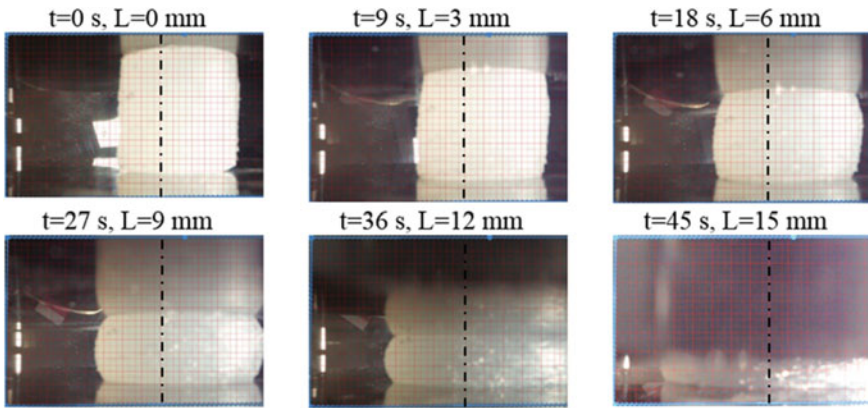


Fig. 38.1 The chosen result of the compression process

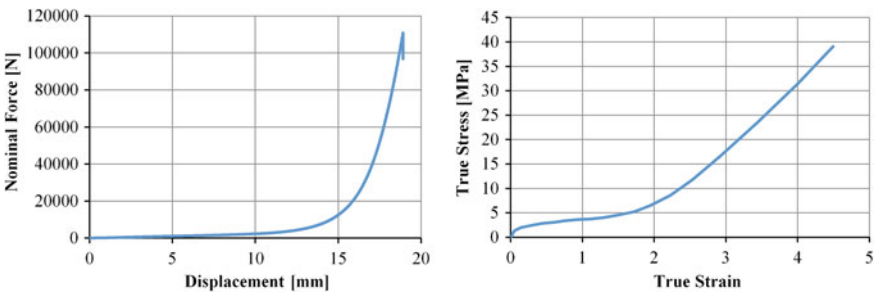


Fig. 38.2 The graphs of the nominal force versus displacement (left) and true stress versus true strain (right)

in the form of disks with the diameter  $D = 23$  mm and two different thicknesses  $L = 3$  and  $1.5$  mm. This allowed different strain rates to be obtained.

Experimental compression tests at high strain rates were performed on the conventional SHPB apparatus (see Fig. 38.3).

The apparatus consists of a gas gun, incident and transmission bars (both 2000 mm long) made of V720 maraging steel, an energy absorber, a data acquisition system and a control system. The striker is launched using compressed gas (argon) and impacts the incident bar. The details of this technique are included in [8, 9]. Waves in the incident and transmission bars are sensed by strain gauges (EA-06-060LZ-120, Vishay, USA) which are placed in the middle of the bars. In order to measure pressure bar signals, strain gauges connected in a half bridge configuration are used. The signals from the strain gauges (the Wheatstone bridges) are conditioned with a transient amplifier LTT 500 (LTT Labortechnik Tasler GmbH, Germany) and recorded with a computer and high-speed A/D computer board NI USB-6366 (National Instruments, USA). In the described apparatus, the amplifier and the A/D computer board with

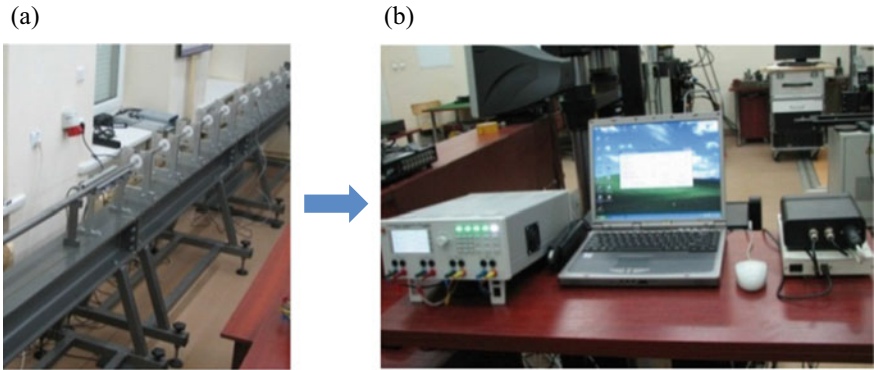


Fig. 38.3 Stand for testing materials at high strain rates: **a** Hopkinson bar system, **b** computer control system

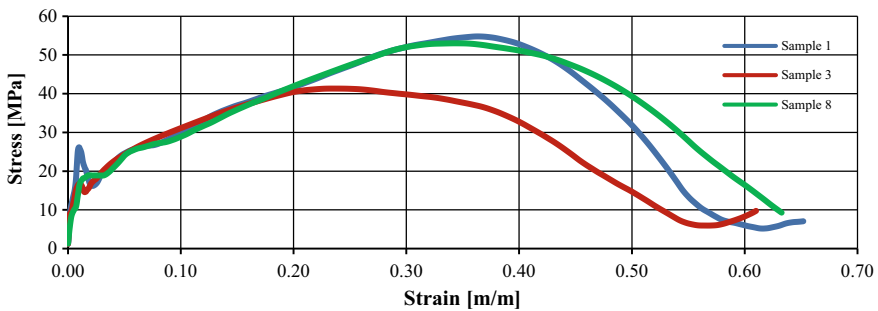
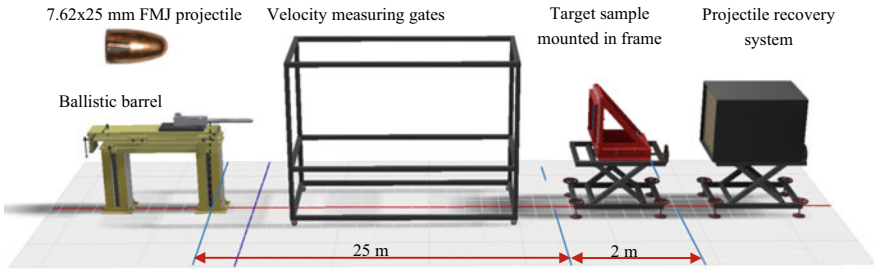


Fig. 38.4 Results of the compression test under high strain rate conditions

1 MHz frequency response are used what allows for accurately recording the transient signals from the strain gauges of the SHPB apparatus. During experimental investigations striker velocities were about 14.0 m/s. Pulse shaping technique was used to shape the profile of the incident pulse. Disks made of rubber with  $D = 8$  mm and  $L = 2$  mm were used as pulse shapers. An exemplary graph obtained in the compression test under high strain rate conditions for chosen samples was shown in Fig. 38.4.

### 38.3 Ballistic Impact Experiments

The behavior of the hyperelastic target material under high strain rate conditions including failure was analyzed during the ballistic impact tests. The scheme of the test stand was shown in Fig. 38.5. Several variants of hyperelastic target with various thickness were tested. The projectile was fired from a ballistic barrel placed in a holder



**Fig. 38.5** The scheme of the ballistic impact test

on a metal platform fixed to the ground. During the ballistic impact tests, the distance between the ballistic barrel and the sample was  $L = 25$  m. The axis of the barrel was perpendicular to the surface of the sample in a vertical and horizontal plane. The sample was mounted in the holder and its edges were fixed by the clamp of the frame (internal dimensions of  $200 \times 200$  mm) tightened with screws. A projectile recovery system was set up at a distance of 2 m behind the sample surface in order to catch the projectiles after perforating the samples. The velocity of the projectile in front of the target was measured by measuring gates. Doppler radar was used to measure residual velocity of projectile after perforation of the target. The results of the ballistic experiments of the  $7.62 \times 25$  mm FMJ projectile impact into plastic targets were shown in Table 38.1 and Fig. 38.6. Three shots were performed for each of target

**Table 38.1** Results of ballistic impact experiments

Target thickness, (mm)	0	10	20	30	80	140	180	220
Residual velocity of projectile, (m/s)*	450	441.5	432.8	426.4	373.2	124.3	45.6	0

\* average value from 3 trials

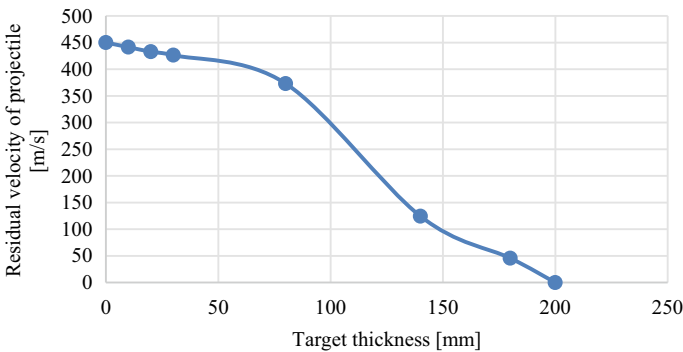
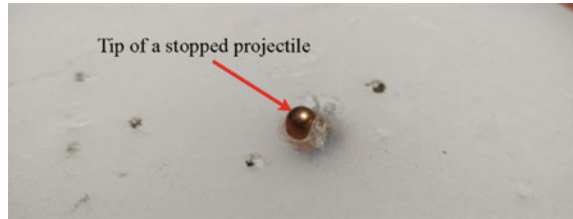


**Fig. 38.6** The graph of the residual velocity versus target thickness

**Fig. 38.7** The example of the 220 mm target deformation after projectile's stopping



variant. The dimensions of the deformed projectiles and their residual velocities after in case of perforation of the target were measured after impact (Fig. 38.6).

Deformations of the targets after the projectile impact were shown in Fig. 38.7.

## 38.4 Conclusions

Various types of experimental tests were carried out in order to determine the response of the novel visco-hyperelastic target to specific loads as well as to define the initial parameters to the numerical model. The plastic behavior at high strain rates was examined, as well as the mechanisms of the material failure depending on the thickness of the layer was analyzed. Residual velocity of projectiles (after perforation of the target) was recorded during the test allowing to evaluate energy absorption and dissipation capability of the plastic layer. On the basis of the data collected during experimental tests the numerical models of  $7.62 \times 25$  mm FMJ projectile and the novel visco-hyperelastic target will be defined. The models will be used in numerical simulations reproduced the experiments performed in the future.

## References

1. Yang H, Yao X, Zheng Z, Gong L, Yuan L, Yuan Y, Liu Y (2018) Highly sensitive and stretchable graphene-silicone rubber composites for strain sensing. *Compos Sci Technol* 167:371–378
2. Pouriaeyali H, Guo Y, Shim V (2011) A visco-hyperelastic constitutive description of elastomer behaviour at high strain rates. *Procedia Eng* 10:2274–2279
3. Tubaldi E, Mitoulis S, Ahmadi H (2018) Comparison of different models for high damping rubber bearings in seismically isolated bridges. *Soil Dyn Earthq Eng* 104:329–345
4. Yang H, Yao X-F, Wang S, Ke Y-C, Huang S-H, Liu Y-H (2018) Analysis and inversion of contact stress for the finite thickness Neo-Hookean layer. *J Appl Mech* 85(10):101008
5. Mabbott A, Carr DJ, Champion S, Malbon C, Tichler C (2013) Comparison of 10% Gelatine, 20% Gelatine and Perma-Gel™ for Ballistic Testing. In: *Proceedings of international symposium on ballistics*, pp 648–654. Lancaster, Freiberg
6. Kalcioğlu ZI, Qu M, Strawhecker KE, Shazly T, Edelman E, VanLandingham MR, Smith JF, Van Vliet KJ (2011) Dynamic impact indentation of hydrated biological tissues and tissue surrogate gels. *Phil Mag* 91(7):1339–1355

7. Bracq A, Haugou G, Delille R, Lauro F, Roth S, Mauzac O (2017) Experimental study of the strain rate dependence of a synthetic gel for ballistic blunt trauma assessment. *J Mech Behav Biomed Mater* 72:138–147
8. Chen W, Song B (2011) Split Hopkinson (Kolsky) Bar. Design, testing and applications, Springer
9. Sharpe WN (2008) Springer handbook of experimental solid mechanics. Springer.
10. Banaszkiwicz M (2016) Analysis of rotating components based on a characteristic strain model of creep. *J Eng Mater Technol Trans ASME* 138(3):031004-1–11
11. Banaszkiwicz M (2019) Creep life assessment method for online monitoring of steam turbine rotors. *Mater High Temp* 36(4):154–367
12. Zeiler G, Bauer R, Putschoegl A (2010) Experiences in manufacturing of forgings for power generation application. *La Metallurgia Italiana* 6:33–40
13. IEC 60045-1 (2020) Steam turbines—part 1: Specifications. International Electrotechnical Commission, 2nd edn